Journal of Cybernetics and Informatics

published by

Slovak Society for Cybernetics and Informatics

Volume 8, 2009

http://www.sski.sk/casopis/index.php (home page)

ISSN: 1336-4774

Journal of Cybernetics and Informatics 8 (2009)
http://www.sski.sk/casopis/index.php

BACKSTEPPING PROPULSION SYSTEM CONTROL FOR ELECTRIC VEHICLE DRIVE

Abdelfatah Nasri[1], Abdeldjabar Hazzab[1], Ismail.K Bousserhane[1], Samir Hadjeri[2] and Pièrre Sicard[3]

[1]University of Bechar, Departement of Electrical Engineering, B.P 417 BECHAR (08000), Algeria.
[2] University of Djillali Liabes, B.P 98 Sidi Bel-Abbes (22000), Algeria.
[3]Group of research in industrial electronics, University of Quebec at Three Rivers, Canada.
e-mails: nasriab1978@yahoo.fr, a_hazzab@yahoo.fr, Bou_isma@yahoo.fr, Pierre.Sicard@uqtr.ca, shadjeri2@yahoo.fr.

Abstract

Nowadays the uses of electrical power resources are integrated in the modern vehicle motion traction chain so new technologies allow the development of electric vehicles (EV) by means of electric motors association with static converters. All mechanical transmission devices are eliminated and vehicle wheel motion can be controlled by means of power electronics. The proposed propulsion system consists of two induction motors (IM) that ensure the drive of the two back driving wheels. The proposed control structure-called independent machines- for speed control permit the achievement of an electronic differential. The electronic differential system ensures the robust control of the vehicle behavior on the road. It also allows controlling, independently, every driving wheel to turn at different speeds in any curve. This paper presents the study and the design of the Backstepping control strategy of the electric vehicle driving wheel. Our electric vehicle feed-Back control's simulated in MATLAB SIMULINK environment, the results obtained present the efficiency of the proposed control with no overshoot, the rising time is perfected with good disturbances rejections comparing with the classical control law.

Keywords: Electric vehicle, traction chain, driving wheels, Backstepping control, propulsion system

1 INTRODUCTION

Electric vehicles (EVs) are developing fast during this decade due to drastic issues on the protection of environment and the shortage of energy sources. While commercial hybrid cars have been rapidly exposed on the market, fuel-cell-powered vehicles are also announced to appear in 5–10 years. Researches on the power propulsion system of EVs have drawn significant attention in the automobile industry and among academics. EVs can be classified into various categories according to their configurations, functions or power sources. Pure EVs do not use petroleum, while hybrid cars take advantages of energy management between gas and electricity [1].Indirectly driven EVs are powered by electric motors through transmission and differential gears, while directly driven vehicles are propelled by in-wheel or, simply, wheel motors [2]. The basic vehicle configurations of this research has two directly driven wheel motors installed and operated inside the driving wheels on a pure EV. These wheel motors can be controlled independently and have so quick and accurate response to the command that the vehicle chassis control or motion control becomes more stable and robust, compared to indirectly driven EVs. Like most research on the torque distribution control of wheel motor, wheel motors [3] proposed a dynamic optimal tractive force distribution control for an EV driven by four wheel motors, thereby improving vehicle handling and stability.

The researchers assumed that wheel motors were all identical with the same torque constant; neglecting motor dynamics the output torque was simply proportional to the input current with a prescribed torque constant. In this paper, a Backstepping decoupling controller for electric vehicle speed control is proposed. The reminder of this paper is organized as follows. Section (2) reviews the principle components of the Electric traction chain with their equations model. Section (3) shows the direct field-oriented control (FOC) of induction motor. Section (4) shows the development of Backstepping controllers design for Electric vehicle .The proposed structure of the studied propulsion system is given in the section (5). Section (6) gives some simulation results of the different studied cases. Finally, the conclusion is drawn in section (7).

2 ELECTRIC TRACTION SYSTEM ELEMENTS MODELLING

Fig. 1 represents the general diagram of an electric traction system using an induction motor (IM) supplied by voltage inverter [4, 8].

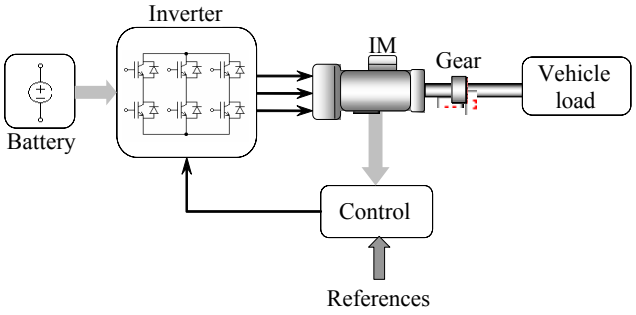

Figure 1: Electrical traction chain

2.1 Energy Source

The battery considered in this paper is of the Lithium-Ion [9], the battery current is calculated by:

$$I_{bat} = \frac{V_{oc} - \sqrt{V_{oc}^2 - 4.(R_{int} + R_t).P_b}}{2.(R_{int} + R_t)} \quad (1)$$

Where:

P_b : Output power of battery
R_{int}: Internal resistance
V_{oc}: The open circuit voltage
R_t : The terminal voltage of the battery

2.2 Static Converter

In this electric traction system, we use a three balanced phases of alternating current inverter with variable frequency from the current battery [4].

$$\begin{bmatrix} v_{an} \\ v_{bn} \\ v_{cn} \end{bmatrix} = \frac{U_{dc}}{2} \begin{bmatrix} 2 & -1 & -1 \\ -1 & 2 & -1 \\ -1 & -1 & 2 \end{bmatrix} \begin{bmatrix} S_a \\ S_b \\ S_c \end{bmatrix} \quad (2)$$

The S_i are logical switches obtained by comparing the control inverter signals with the modulation signal.

2.3 Traction Motor

The used motorization consist of three phase induction motor (IM) supplied by a voltage inverter controlled by Pulse Width Modulation (PWM) techniques. The dynamic model of three-phase, Y-connected induction motor can be expressed in the d-q synchronously rotating frame as [4, 6, 13]

$$\begin{cases} \dfrac{di_{ds}}{dt} = \dfrac{1}{\sigma.L_s}.\left(-\left(R_s + \left(\dfrac{L_m}{L_r}\right)^2.R_r \right).i_{ds} + \sigma.L_s.\omega_e.i_{qs} + \dfrac{L_m.R_r}{L_r^2}.\varphi_{dr} + \dfrac{L_m}{L_r}.\varphi_{qr}.\omega_r + V_{ds} \right) \\ \dfrac{di_{qs}}{dt} = \dfrac{1}{\sigma.L_s}.\left(-\sigma.L_s.\omega_e.i_{ds} - \left(R_s + \left(\dfrac{L_m}{L_r}\right)^2.R_r \right).i_{qs} - \dfrac{L_m}{L_r}.\varphi_{dr}.\omega_r + \dfrac{L_m.R_r}{L_r^2}.\varphi_{qr} + V_{qs} \right) \\ \dfrac{d\varphi_{dr}}{dt} = \dfrac{L_m.R_r}{L_r}.i_{ds} - \dfrac{R_r}{L_r}.\varphi_{dr} + (\omega_e - \omega_r).\varphi_{dr} \\ \dfrac{d\varphi_{qr}}{dt} = \dfrac{L_m.R_r}{L_r}.i_{qs} - (\omega_e - \omega_r).\varphi_{dr} - \dfrac{R_r}{L_r}.\varphi_{qr} \\ \dfrac{d\omega_r}{dt} = \dfrac{3}{2}\dfrac{P^2.L_m}{L_r.J}.(i_{qs}.\varphi_{dr} - i_{ds}.\varphi_{qr}) - \dfrac{f_c}{J}.\omega_r - \dfrac{P}{J}.T_l \end{cases} \tag{3}$$

Where σ is the coefficient of dispersion and is given by (3):

$$\sigma = 1 - \frac{L_m^2}{L_s L_r} \tag{4}$$

L_s, L_r, L_m	stator, rotor and mutual inductances;
R_s, R_r	stator and rotor resistances;
ω_e, ω_r	electrical and rotor angular frequency;
ω_{sl}	slip frequency $(\omega_e - \omega_r)$;
τ_r	rotor time constant (L_r/R_r);
P	pole pairs

2.4 Mechanical Part

The developed globally traction chain model based on the data uses from the Leroy-Somer Society, [4] is shown in Fig. 2:

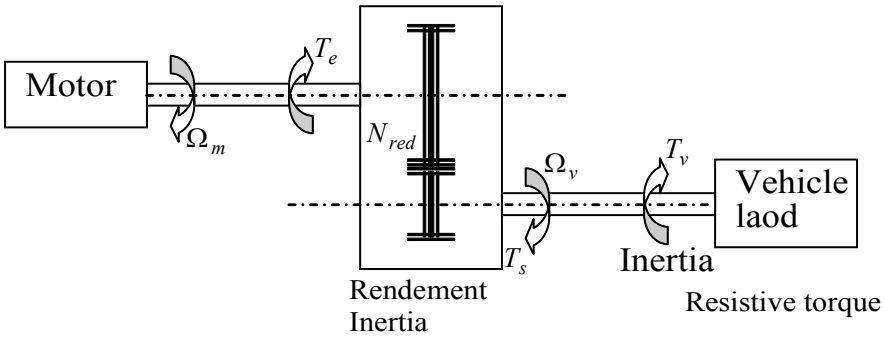

Figure 2: Electromechanical structure

2.4.1 The Vehicle As Load

The vehicle is considered as a load is characterized by many torques which are mostly considered as resistive torques [4, 5, 12, 15, 17, 18]. The different torques includes:

- The vehicle inertia torque defined by the following relationship:

$$T_{in} = J_v . \frac{dw_v}{dt} \tag{5}$$

- The aerodynamics torque is :

$$T_{aero} = \frac{1}{2} \rho S.T_x .R_r^3 .w_r^2 \tag{6}$$

- The slope torque is :

$$T_{slope} = Mg.\sin\alpha \tag{7}$$

The maximal torque of the tire which can be opposed to the motion has the following expression:

$$T_{tire} = Mgf_r .R_r \tag{8}$$

We obtain finally the total resistive torque:

$$T_v = T_{slope} + T_{tire} + T_{aero} \tag{9}$$

2.4.2 Gear

The speed gear ensures the transmission of the motor torque to the driving wheels. The gear is modelled by the gear ratio, the transmission efficiency and its inertia.

The mechanical equation is given by:

$$J_e \frac{dw_m}{dt} + fw_m = p(T_{em} - T_r) \tag{10}$$

With:

$$T_r = \frac{1}{\eta N_{red}} T_v \tag{11}$$

$$J_e = J + \frac{J_v}{\eta N_{red}^2} \tag{12}$$

The modelling of the traction system allows the implementation of some controls such as the vector control and the speed control in order to ensure the globally system stability.

3. VECTOR CONTROL

The main objective of the vector control of induction motors is, to control independently the flux and he torque as DC machines, this is done by using a d-q rotating reference frame synchronously with the rotor flux space vector [6, 7]. In ideally field-oriented control, the rotor flux linkage axis is forced to align with the d-axes, and it follows that [7, 10, 13, 14]:

$$\varphi_{rq} = \frac{d\varphi_{rq}}{dt} = 0 \tag{13}$$

$$\varphi_{rd} = \varphi_r = constant \tag{14}$$

Applying the result of (13) and (14), namely the indirect field-oriented control, the torque equation become analogous to the DC machine and can be described as follows:

$$T_e = \frac{3}{2}\frac{p \cdot L_m}{L_r} \cdot \varphi_r \cdot i_{qs} \tag{15}$$

And the slip frequency can be given as follow:

$$\omega_{sl} = \frac{1}{\tau_r}\frac{i_{qs}^*}{i_{ds}^*} \tag{16}$$

Consequently, the dynamic equations (3) yield:

$$\begin{cases} \dfrac{di_{ds}}{dt} = -\left(\dfrac{R_s}{\sigma L_s} + \dfrac{1-\sigma}{\sigma\tau_r}\right) i_{ds} + \omega_e i_{qs} + \dfrac{L_m}{\sigma L_s L_r \tau_r}\phi_{rd} + \dfrac{1}{\sigma L_s} V_{ds} \\ \dfrac{di_{qs}}{dt} = -\left(\dfrac{R_s}{\sigma L_s} + \dfrac{1-\sigma}{\sigma\tau_r}\right) i_{qs} - \omega_e i_{ds} + \dfrac{L_m}{\sigma L_s L_r \tau_r}\phi_{rd} + \dfrac{1}{\sigma L_s} V_{ds} \\ \dfrac{d\phi_r}{dt} = \dfrac{L_m}{\tau_r} i_{ds} - \dfrac{1}{\tau_r}\phi_{rd} \\ \dfrac{d\omega_r}{dt} = \dfrac{3}{2}\dfrac{P^2 L_m}{J L_r} i_{qs}\phi_{rd} - \dfrac{f_c}{J}\omega_r - \dfrac{P}{J}T_l \end{cases} \tag{17}$$

Using (12) and (13) the desired flux in terms of ids can be found from:

$$\varphi_{dr} = \frac{L_m / T_r}{s + 1/T_r} \tag{18}$$

The decoupling control method with compensation is to choose inverter output voltages such that [6]:

$$V_{ds}^* = \left(K_p + K_i \frac{1}{s}\right)\left(i_{ds}^* - i_{ds}\right) - \omega_e \sigma L_s i_{qs}^* \tag{19}$$

$$V_{qs}^* = \left(K_p + K_i \frac{1}{s}\right)\left(i_{qs}^* - i_{qs}\right) + \omega_e \sigma L_s i_{ds}^* + \omega_r \frac{L_m}{L_r}\varphi_{rd} \tag{20}$$

According to the above analysis, the direct field-oriented control (DFOC) [2,3,6] of induction motor with current-regulated PWM drive system can reasonably presented by the block diagram shown in the Fig. 3, as first time we choose the classical regulators for field oriented control.

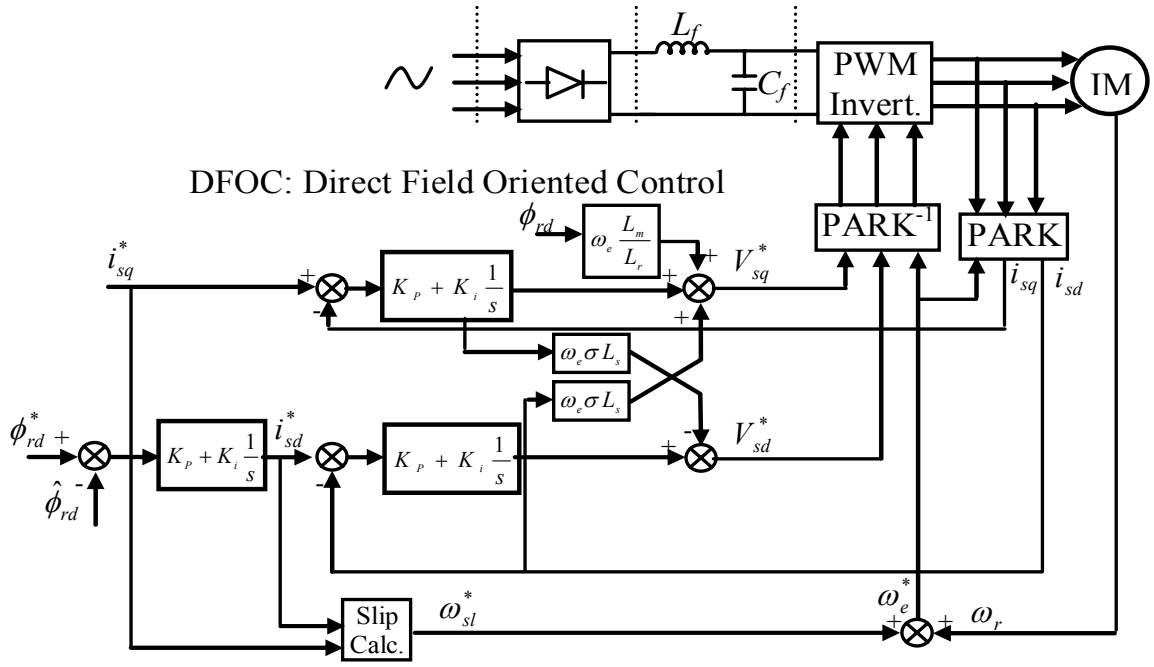

Figure 3: Block diagram of DFOC for an induction motor

4 THE SPEED CONTROL OF THE IM USING BACKSTEPPING TECHNIQUE

4.1 Backstepping Technique

Consider the system:

$$\dot{x} = f(x) + g(x)u\,,\ f(0) = 0 \tag{21}$$

Where $x \in R^n$ is the state and $u \in R$ is the control input. Let $u_{des} = \alpha(x),\ a(0) = 0$ be the desired feedback control law, which, if it's applied to the system in (21), it's ensure the globally boundedness and regulation of $x(t)$ to the equilibrium point $x = 0$ as $t \to \infty$, for all $x(0)$ and $V(x)$ is a control Lyapunov function, where :

$$\frac{\partial V(x)}{\partial x}\left[f(x) + g(x)\alpha(x)\right] < 0\,,\ V(x) > 0 \tag{22}$$

Consider the following cascade system:

$$\dot{x} = f(x) + g(x)y\,,\ f(0) = 0 \tag{23}$$

$$\dot{\zeta} = m(x,\zeta) + \beta(x,\zeta)u\,,\ h(0) = 0 \tag{24}$$

$$y = h(x) \tag{25}$$

Where for the system in (23), a desired feedback $a(x)$ and a control Lyapunov function *V(x)* are known. Then, using the nonlinear block backstepping theory in [10, 11, 14, 18], the error between the actual and the desired input for the system in (23) can be defined as $z = y - \alpha$, and an overall control Lyapunov function $V(x,\zeta)$ for the systems in (23) and (24) can be defined by augmenting a quadratic term in the error variable z with $V(x)$:

$$V(x,\zeta) = V(x) + \frac{1}{2}z^2 \tag{26}$$

Taking the derivative of both sides gives:

$$\dot{V}(x,\zeta)=\dot{V}(x)+z\dot{z} \tag{27}$$

The aim objective is to have practical solutions of $u(x,\zeta)$ and in other hand to get $\dot{V}(x,\zeta)$ negative, yields a feedback control law for the full system in (23-25). One particular choice is [7, 11, 14, 15, 18]:

$$u=\left(\frac{\partial h(\zeta)}{\partial\zeta}\beta(x,\zeta)\right)^{-1}\left\{-c(y-\alpha)-\frac{\partial h(\zeta)}{\partial\zeta}m(x,\zeta)+\frac{\partial\alpha(x)}{\partial x}\dot{x}-\frac{\partial V(x)}{\partial x}g(x)\right\},\quad c>0 \tag{28}$$

4.2 Application to Induction Motor

In this section we use the Backstepping algorithm to develop the speed control law of the induction motor. This speed will converge to the reference value from a wide set of initial conditions.

Step 1:

Firstly we consider the tracking objective of the direct current (φ_{dr}). A tracking error $z_1=\varphi_{dr}^{*}-\varphi_{dr}$ is defined and the derivative becomes:

$$\dot{z}_1=\frac{d\varphi_{dr}^{*}}{dt}-\frac{R_r}{L_r}\cdot\left(L_m\cdot i_{ds}-\varphi_{dr}\right) \tag{29}$$

To initiate Backstepping, we prpose i_{ds} as a first virtual control. If the function stability is proposed as:

$$i_{ds}^{*}=\frac{\varphi_{dr}}{L_m}+c_1\cdot\frac{\tau_r}{L_m}\cdot z_1+\tau_r\cdot\frac{d\varphi_{dr}}{dt} \tag{30}$$

We obtain:

$$\dot{z}_1=c_1\cdot z_1+\frac{1}{\tau_r}\cdot\left(i_{ds}-i_{ds}^{*}\right) \tag{31}$$

Due to the fact that i_{ds} is not a control input an error variable $z_2=i_{ds}-i_{ds}^{*}$ is defined and we have the derivative as follows:

$$\dot{z}_2=c_1\cdot z_1+\frac{1}{\tau_r}\cdot z_2 \tag{32}$$

Step 2:

The derivative of the error variable $z_2=i_{ds}-i_{ds}^{*}$ is:

$$\begin{aligned}\dot{z}_2=&-\frac{L_m}{\tau_r}\cdot\left(L_m\cdot i_{ds}-\varphi_{dr}\right)+c_1\cdot\left(i_{ds}-\frac{\varphi_{dr}}{L_m}-\tau_r\cdot\frac{d\varphi_{dr}^{*}}{dt}\right)-\frac{\tau_r}{L_m}\cdot\frac{d^2\varphi_{dr}}{dt^2}+\frac{1}{\sigma\cdot L_s}\cdot V_{ds}\\&-\frac{1}{\sigma\cdot L_s}\left(R_r\cdot i_{ds}-w_e\cdot\sigma\cdot L_s\cdot i_{qs}+\left(\frac{L_m}{L_r}\right)^2\cdot R_r\cdot\left(i_{ds}-\frac{\hat{\varphi}_{dr}}{L_m}\right)\right)\\&+\frac{\left(\frac{L_m}{L_r}\right)^2\cdot R_r}{\sigma\cdot L_s}\cdot\frac{\varphi_{dr}}{L_m}+w_r\cdot\frac{L_m}{\sigma\cdot L_s\cdot L_r}\cdot\varphi_{qr}\end{aligned} \tag{33}$$

Viewing φ_{dr} and φ_{qr} as unknown disturbances we apply nonlinear damping [10, 14, 18] to design

the control function:

$$\frac{1}{\sigma \cdot L_s} \cdot V_{sd} = \frac{1}{\sigma \cdot L_s}\left(R_s \cdot i_{ds} - w_e \cdot \sigma \cdot L_s \cdot i_{qs} + \left(\frac{L_m}{L_r}\right)^2 \cdot R_r \cdot \left(i_{ds} - \frac{\hat{\varphi}_{dr}}{L_m} \right) \right)$$
$$\cdot \left(\frac{1}{\tau_r} - c_1 \right) \cdot \left(i_{ds} - \frac{\hat{\varphi}_{dr}}{L_m} \right) + c_1 \frac{\tau_r}{L_m} \cdot \frac{d\varphi^*_{dr}}{dt} + \frac{\tau_r}{L_m} \cdot \frac{d^2\varphi^*_{dr}}{dt^2} \tag{34}$$
$$- c_2 \cdot z_2 - \frac{1}{\tau_r} \cdot z_1 - d_2 \cdot \left\{ \left(\frac{(L_m/L_e)^2 R_r}{\sigma L_s} \right)^2 + \left(w_r \cdot \frac{(1-\sigma)}{\sigma} \right)^2 \right\} \cdot z_2$$

We define:

$$\varphi_1 = \frac{\left(\frac{L_m}{L_r}\right)^2 \cdot R_r}{\sigma \cdot L_s}, \qquad \varphi_2 = w_r \cdot \frac{\frac{L_m^2}{L_r}}{\sigma \cdot L_s} \qquad \text{and} \qquad \varphi^2 = \varphi_1^2 + \varphi_2^2 .$$

The insertion of the control function in the dynamics of the variable error z_2 gives:

$$\dot{z}_2 = -c_2 \cdot z_2 - \frac{1}{\tau_r} z_1 - d_2 \cdot \varphi^2 \cdot z_2 + \varphi_1 \cdot \frac{\varphi_{dr}}{L_m} + \varphi_2 \cdot \frac{\varphi_{qr}}{L_m} \tag{35}$$

Step 3:

We now search to find the torque tracking error. The tracking error is for $\varphi_{dr} \neq 0$ defined as:

$$z_3 = i_{qs} - \frac{T_e^*}{\left(P \cdot \frac{L_m}{L_r} \cdot \varphi_{dr} \right)} \tag{36}$$

Then, its derivative is:

$$\dot{z}_3 = \frac{1}{\sigma \cdot L_s} \cdot V_{qs} - \frac{1}{\sigma \cdot L_s} \cdot \left(R_s \cdot i_{sq} + w_e \cdot \sigma \cdot L_s \cdot i_{ds} + \left(\frac{L_m}{L_r}\right)^2 \cdot R_r \cdot i_{qs} \right.$$
$$\left. + w_r \cdot (1-\sigma) \cdot L_s \cdot \frac{\hat{\varphi}_{dr}}{L_m} \right) - \frac{\left(\frac{L_m}{L_r}\right)^2 \cdot R_r}{\sigma \cdot L_s} \cdot \frac{\varphi_{qr}}{L_m} + w_r \cdot \frac{\frac{L_m^2}{L_r}}{\sigma \cdot L_s} \cdot \frac{\varphi_{dr}}{L_m} \tag{37}$$
$$+ \frac{L_r \cdot T_e^*}{P \cdot \varphi_{dr}^2} \cdot \frac{1}{\tau_r} \cdot \left(i_{ds} - \frac{\hat{\varphi}_{dr}}{L_m} \right) - \frac{L_r}{P \cdot L_m \cdot \hat{\varphi}_{dr}} \cdot \frac{dT_e^*}{dt}$$

Viewing φ_{dr} and φ_{qr} as unknown disturbances we apply nonlinear damping [14, 15, 18] to design the control function:

$$\frac{1}{\sigma \cdot L_s} \cdot V_{qs} = \frac{1}{\sigma \cdot L_s} \cdot \left(R_s \cdot i_{qs} - w_e \cdot \sigma \cdot L_s \cdot i_{qs} + \left(\frac{L_m}{L_r} \right)^2 \cdot R_r \cdot i_{qs} \right.$$
$$\left. + w_r \cdot (1-\sigma) \cdot L_s \cdot \frac{\hat{\varphi}_{dr}}{L_m} \right) - \frac{2 \cdot L_r \cdot T_e^*}{3 \cdot P \cdot \varphi_{dr}} \cdot \frac{1}{T_r} \cdot \left(i_{ds} - \frac{\hat{\varphi}_{dr}}{L_m} \right) + \frac{2 \cdot L_r}{3 \cdot P \cdot L_m \cdot \hat{\varphi}_{dr}} \cdot \frac{dT_e^*}{dt} \tag{38}$$
$$- c_3 \cdot z_3 - d_3 \cdot \left\{ \left(\frac{\left(\frac{L_m}{L_r} \right)^2 \cdot R_r}{\sigma \cdot L_s} \right)^2 + \left(w_r \cdot \frac{(1-\sigma)}{\sigma} \right)^2 \right\} \cdot z_3$$

The insertion of the control function in the dynamics of the variable error z_3 gives:

$$\dot{z}_3 = -c_3 \cdot z_3 - d_3 \cdot \varphi^2 \cdot z_3 + \varphi_1 \cdot \frac{\varphi_{qr}}{L_m} + \varphi_2 \cdot \frac{\varphi_{dr}}{L_m} \tag{39}$$

The combined controller is shown in Fig.4 where we have:

$$\begin{cases} V_{ds,ff} = R_s \cdot i_{ds} - \omega_s \cdot \sigma \cdot L_s \cdot i_{qs} + \left(\frac{L_m}{L_r} \right)^2 \cdot R_r \cdot \left(i_{ds} - \frac{\hat{\varphi}_{dr}}{L_m} \right) \\ V_{qs,ff} = R_s \cdot i_{sq} - \omega_s \cdot \sigma \cdot L_s \cdot i_{qs} + \left(\frac{L_m}{L_r} \right)^2 \cdot R_r \cdot i_{sq} + \omega_r \cdot (1-\sigma) \cdot L_s \cdot \frac{\hat{\varphi}_{dr}}{L_m} \\ V_{ds,nl} = \sigma \cdot L_s \cdot \left\{ \left(\frac{1}{\tau_r} - c_1 \right) \cdot \left(i_{ds} - \frac{\hat{\varphi}_{dr}}{L_m} \right) - \frac{1}{L_m \cdot \tau_r} \left(\hat{\varphi}_{dr} - \varphi_{dr}^* \right) \right\} \\ V_{qs,nl} = -\frac{2 \cdot L_m^2 \cdot T_{em}^*}{3 \cdot P \cdot (1-\sigma) \cdot L_s \cdot \varphi_{dr}^2} \cdot \frac{\sigma \cdot L_s}{\tau_r} \cdot \left(i_{ds} - \frac{\hat{\varphi}_{dr}}{L_m} \right) \end{cases} \tag{40}$$

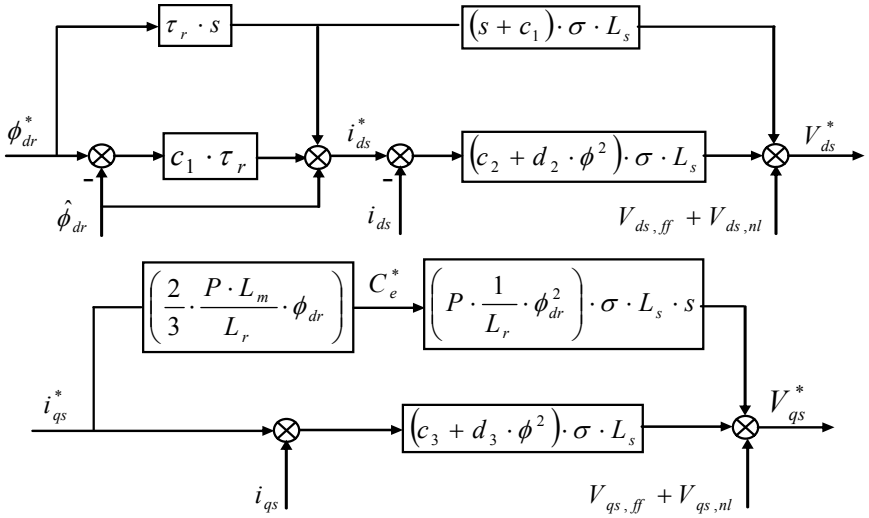

Figure 4: Nonlinear field-oriented control of Electric Vehicle IM using Backstepping technique

4.3 Speed Control of Electric Vehicle Induction Motor's Using Backstepping Strategy

To control the speed of the vehicle motorization, we find to search the error speed tracking. We consider that i_{qs}^{*} is the control law, so tracking error is defined as:

$$z_0 = \omega_r^{*} - \omega_r \tag{41}$$

So, its derivate is given as:

$$\dot{z}_0 = \dot{\omega}_r^{*} - \dot{\omega}_r \tag{42}$$

$$\dot{z}_0 = \dot{\omega}_r^{*} - \left[\frac{3}{2} \frac{P^2 \cdot L_m}{L_r \cdot J} \cdot i_{qs} \cdot \varphi_{dr} - \frac{f_c}{J} \cdot \omega_r - \frac{P}{J} \cdot T_l \right] \tag{43}$$

The control law obtained is :

$$i_{qs}^{*} = \frac{2}{3} \frac{L_r \cdot f_c}{P^2 \cdot L_m \cdot \varphi_{dr}} \cdot \omega_r + c_0 \frac{2 \cdot L_r \cdot J}{3 \cdot P^2 \cdot L_m \cdot \varphi_{dr}} z_0 + \frac{2}{3} \frac{L_r}{P \cdot L_m} \cdot T_l \tag{44}$$

5 STRUCTURE OF THE STUDIED SYSTEM

The general scheme of the driving wheels control is represented by Fig. 5. It is an electric vehicle, the back driving wheels are controlled independently by two IM. The reference blocks must provide the speed references of each motor taking into account information from the different sensors.

- **Speed References Computation**

It's possible to determine the speed references according to the decision of the driver. When the vehicle arrives at the beginning of a curve, the driver applies a curve angle on each driving wheel [12, 13, 16, 17, 18]. The electronic differential acts immediately on the two motors reducing the driving wheel speed situated inside the curve, and increases the speed of the driving wheel situated outside the curve. The angular speeds of the driving wheels are:

$$w_{rR} = \frac{V_h}{R_r} + k_b . \Delta w \tag{45}$$

$$w_{rL} = \frac{V_h}{R_r} - k_b . \Delta w \tag{46}$$

With k_b = +1 corresponding to a choice of the direction of the wheel, (-1) for the right turn, and (+1) for the left turn. The driving wheels speeds variation's is imposed by the trajectory desired by the driver and is given by:

$$\Delta w = \frac{d_w}{2} \frac{sin(\delta + \beta)}{l_w . cos\,\delta} . \frac{V_h}{R_r} \tag{47}$$

The relation between α which the curve angle given by the driver wheel and δ the real curve angle of the wheels is given by:

$$\delta = \frac{\alpha}{k_d} \tag{48}$$

The Fig. 6 shows the vehicle geometry of the studied system.

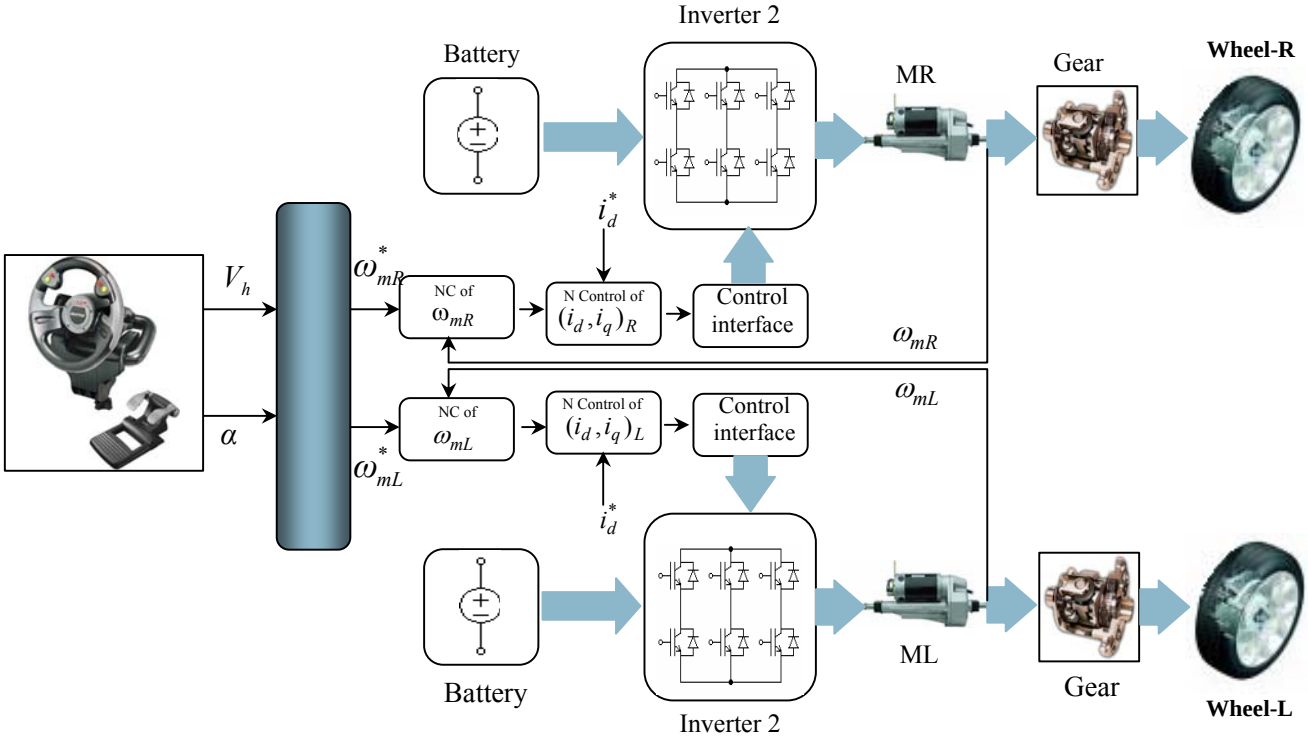

Figure 5: The driving wheels nonlinear control (Backstepping) system.

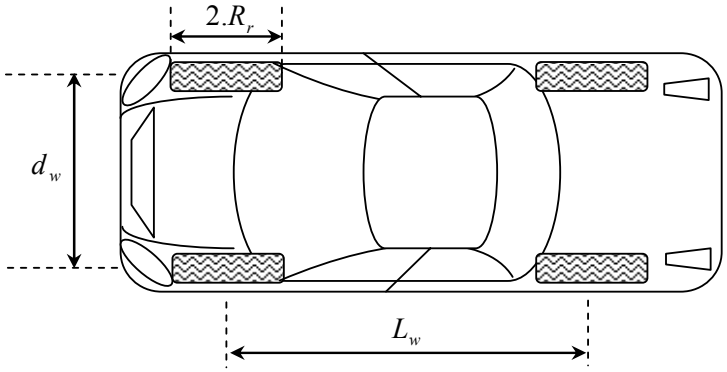

Figure 6: Vehicle geometry

Where k_d is the gear ratio. A proportionality coefficient between δ and β the vehicle slip angle is defined as:

$$\beta = k.\delta \tag{49}$$

The speeds references of the two motors are:

$$w_{mR}^* = N_{red}.w_{rR} \tag{50}$$

$$w_{mL}^* = N_{red}.w_{rL} \tag{51}$$

6 SIMULATION RESULTS

In order to characterise the driving wheel system behavior, simulations were carried using the model of Fig. 5. They show vehicle speed variation for two types of controllers, PI and the Backstepping controller.

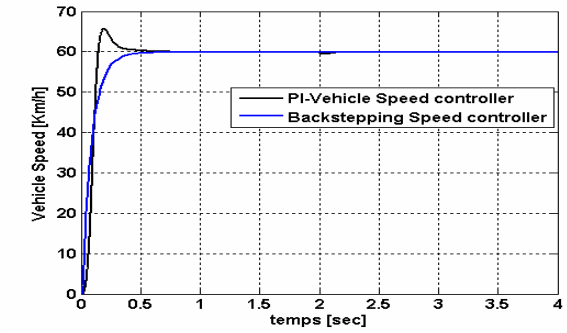

Figure 7.1: Vehicle speed for two controllers

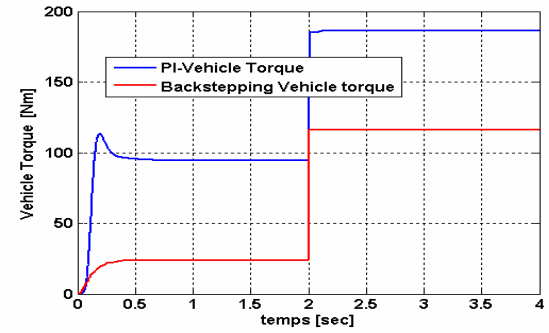

Figure 7.2: Vehicle torque in the two cases

Table I: Performances of the PI and Backstepping controllers in the speed loop response

Results	*Rising time [Sec]*	*Overtaking [%]*	*Steady state error [%]*	*slope torque application time*
PI	0.1564	11.6666	0	At 2 Sec
Backstepping	0.48112	0	0	At 2 Sec

In order to simplify the control algorithm and to improve the control loop robustness, instead of using classical control, we use the Backstepping controller [18]. The advantage of this control law is its robustness, its capacity to maintain ideal trajectories of two wheels independently and the disturbances rejections efficiency with good rising time and good speed response loop and a perfected propulsion system against road parameters variations and vehicle torque parameter optimized and maintaining the system stability. To compare the effect of disturbances on the speed loop and resistive torques in the cases of two control laws, Fig. 7.1, 7.2 shows the system response in two cases. These figures show that the effect of the disturbance is neglected in the case of the Backstepping control. It appears clearly that the classical PI controller is easy to applied, however the control with Backstepping controller offers better performances in both control and tracking error. In addition to these dynamic performances, it respects the imposed constraints by the driving system such as the robustness of parameter variations.

6.1 Case of Straight Way

- Flat road with 10% slope at 60km/h speed

In this test, the system is submitted to the same speed step. The driving wheels speeds stay always the same and the road slope does not affect the control law of the driving wheel. Only a change of the developed motor torque is noticed. The slope sensitize the motorization to develop more and more effort to satisfy the traction chain demand , as a results of the electromagnetic traction motor torque left and right improvement of each motor. The system behavior is illustrated by Fig. 8.1, 8.3, 8.4. The resistive torques are shown in Fig. 8.2.

Table II: Performances of the PI and Backstepping controllers in vehicle speed loop

Results	Δw	V^*_{refL}	V^*_{refR}	α	Vh	V_{wL}	V_{wR}
PI	0	60	60	0	60	59.87	59.87
Backstepping	0	60	60	0	60	60	60

Table III: Performances of the Backstepping and PI controllers

Results	*Total vehicle torques (T_v)*	*Tire torque (Ttire)*	*Aerodynamique torque (Taero)*	*Slope torque (Tslope)*
Maximum value – Backstepping [Nm]	124.80	9.067	23.43	92.26
Maximum value –PI [Nm]	195.00	9.067	93.7	92.26
Time application [Sec]	Permanent	Permanent	Permanent	2

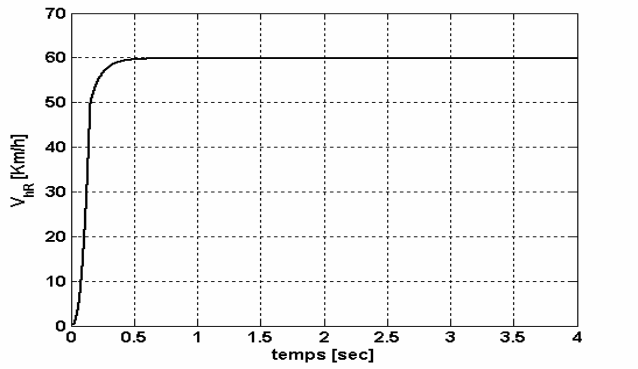

Figure 8.1: Vehicle wheel speed

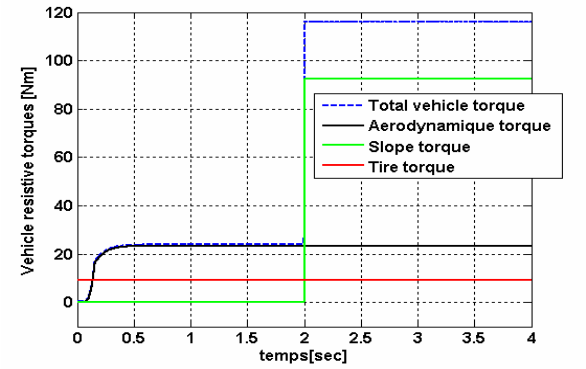

Figure 8.2: Resistive torques

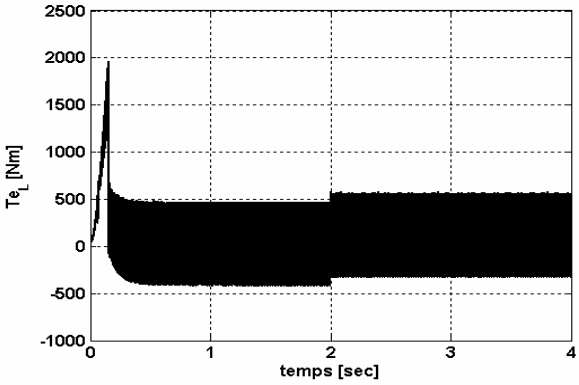

Figure 8.3: Left motor electromagnetic torque

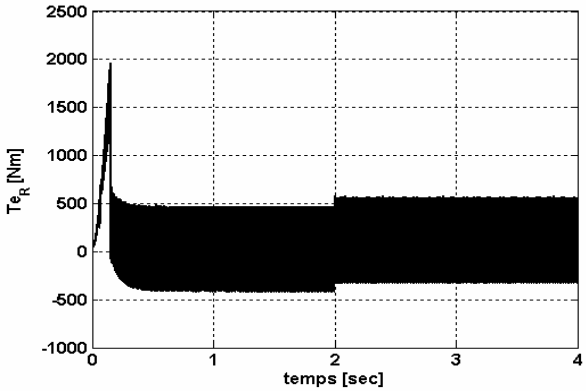

Figure 8.4: Right motor electromagnetic torque

6.2 Case of curved way

- Curved road at right side with speed of 60km/h

The vehicle is driving on a curved road on the right side with 60*km*/*h* speed. The assumption is that the two motors are not disturbed. In this case the driving wheels follow different paths, and they turn in the same direction but with different speeds. The electronic differential acts on the two motor speeds by decreasing the speed of the driving wheel on the right side situated inside the curve, and on the other hand by increasing the wheel motor speed in the external side of the curve. The behavior of these speeds and torques are given by Fig. 9.3, 9.4 respectively, the Fig. 9.1, 9.2 shows the electromagnetic torque left and right variations.

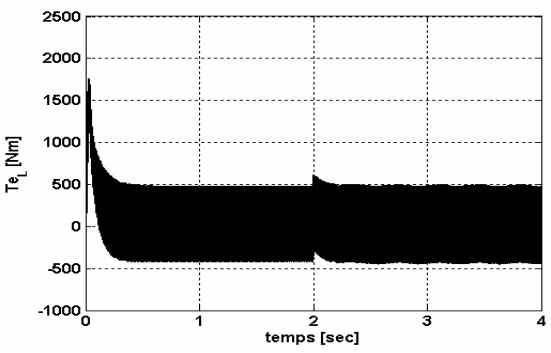

Figure 9.1: Left motor electromagnetic torque

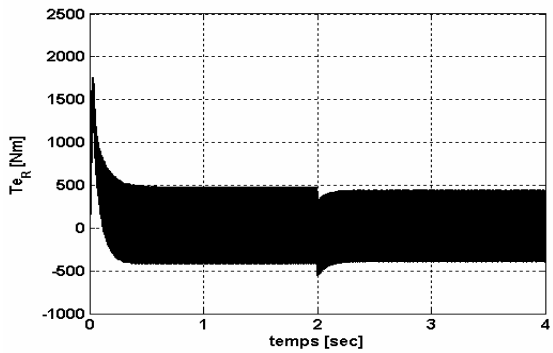

Figure 9.2: Right motor electromagnetic torque

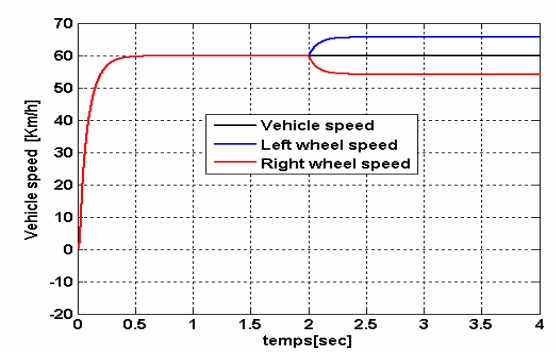

Figure 9.3: Vehicle speed in right turn in curved way

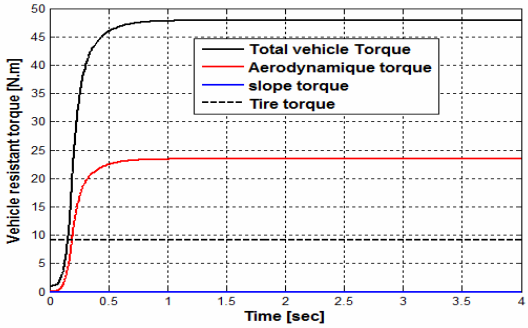

Figure 9.4: Resistive torques in right turn in curved way

Table IV: Performances of the Backstepping controller in the vehicle speed loop

Results	Δv [Km/h]	V^*_{refL} [Km/h]	V^*_{refR} [Km/h]	Time curve [Sec]	Curve angle α [°]	Vh [Km/h]	V_{wL} [Km/h]	V_{wR} [Km/h]
PI	5	65.74	54.26	2	5.81	60	65.6	54.15
Backsteppin	5	65	55	2	5.81	60	65	55

Table V: Performances of the Backstepping and PI controllers on the vehicle torques response

Results	***Total vehicle torques (T_v)***	***Tire torque (Ttire)***	***Aerodynamique torque(Taero)***	***Slope torque (Tslope)***
Maximum value – Backstepping [Nm]	32.54	9.114	23.43	0
Maximum value – PI[Nm]	102.5	9.114	93.7	0
Time application [Sec]	Permanent	Permanent	Permanent	No Application

7 CONCLUSION

In the field of electric drives with variable speed, an application of the electric vehicle controlled by an electronic differential is presented .The research outlined in this paper has demonstrate the feasibility of an improved vehicle stability which utilizes two independent back drive wheels for motion by using the Backstepping control. This paper proposes an 'independent machine's' control structure applied to a propulsion system by the Backstepping speed control law. The results obtained by simulation show that this structure permits the realization of an robust control based on Lyapunov feedback control which ensures good dynamic and static performances, however a good rising time, good disturbance rejection's response with no over shoot.The proposed Backstepping model controls the driving wheels speeds with high accuracy either in flat roads or curved ones and gives more and more safety to the electric vehicle drive in any slope and the disturbances do not affect the performances of the driving motors, the exciting result obtained by the feedback control is the absence of the overshoot and the tracking error.

APPENDIX

Table VI: Electric vehicle Parameters

Te	Motor traction torque	247 Nm

Table VII: Induction Motors Parameters

J_e	Moment on inertia of the drive train	7.07Kgm^2
R_w	Wheel radius	0.36m
a	Total gear ratio	10.0
η	Total transmission efficiency	0.93
M	Vehicle mass	3904Kg
f_e	Bearing friction coefficient	0.001
K_d	Aerodynamic coefficient	0.46
A	Vehicle frontal area	3.48 m^2
f_v	Vehicle friction coefficient	0.01
α	Grade angle of the road	rad
L_w	Distance between two wheels and axes	2.5m
d_w	Distance between the back and the front wheel	1.5m

R_r	Rotor winding resistance (per phase)	0.003 Ω
Rs	Stator winding resistance (per phase)	0.0044 Ω
L_s	Stator leakage inductance (per pohase)	16.1 µH
L_m	Magnetizing inductance (per phase)	482 µH
L_r	Rotor leakage inductance (per phase)	12.9 µH
f_e	Friction coefficient	0.0014
P	Number of poles	4
	Based speed	2885 rpm
	Rated power	100 hp

Table VIII: Symbols, Designation and Units.

Symbols	**Nomenclature**	**units**
J_v	Vehicle inertia	Kg.m^2
T_v	Vehicle torque	Nm
T_{slope}	Slope torque	Nm
T_{aero}	Aerodynamique torque	Nm
T_{tire}	Tire torque	Nm
T_{in}	Inertia vehicle torque	Nm
N_{red}	Report of speed gear	%
G	Gear box	-
NC	Nonlinear Control	-
ρ	Air density	
C_x	Aerodynamic drag coefficient	
g	Gravitational acceleration	N/m
U_{dc}	Battery voltage	Volt
K_b	Choice of direction coefficient	Rad/sec
ΔW	Angular speed variation given by electronic differential	Rad/sec
W_{rR}	Right wheel angular speed	Rad/sec
W_{rL}	Left wheel angular speed	Rad/sec
W^*_{mR}	Right wheel angular speed of reference	Rad/sec
W^*_{mL}	Left wheel angular speed of reference	Rad
δ	Reel angle wheel curve's	Rad
β	Vehicle slip angle	Rad

REFERENCES

[1] A.Poursamad, M. Montazeri."Design of Genetic-Fuzzy Control Strategy for Parallel Hybrid Electric Vehicles ", Control Engineering Practice,doi:10.1016/j.conengprac.2007.10.003.

[2] Y. Pien Yang, C.Pin Lo "Current Distribution Control of Dual Directly Driven Wheel Motor for Electric Vehicles", Control Engineering Practice, Vol n°16, 2008. pp.1285-1292.

[3] He. Hori, Y.Kamachi, M.Walters."Future Motion Control to be realized by in-Wheel Motored Electric Vehicle" .The 31 St Annual Conference of The IEE Industrial Electronics Society .IECON 2005.Raliegh South Carolina, USA.

[4] A.Nasri, A.Hazzab, I.K.Bousserhane, S.Hadjeri, P.Sicard,"Two Wheel Speed Robust Sliding Mode Control For Electric Vehicle Drive ",Serbian Journal of Electrical Engineering , Vol 5,N°2,November 2008 ,PP 199-216.

[5] Multon, B., Hirsinger, L.: Problème de la motorisation d'un véhicule Electrique (Motorization problem of an electric vehicle), EEA " Voiture et Electricité" ("Car and Electricity") 24 et 25 Mars 1994, Cachan (France).

[6] J. Jung, K. Nam, "A Dynamic Decoupling Control Scheme for High-Speed Operation of Induction Motors", IEEE Trans. on Ind. Elect. Vol. 46/01 (1999).

[7] Kanellakopoulos, I., Kokotovic P.V., and Morse, A. S. 'Systematic design of adaptive controller for feedback linearizable systems', IEEE Trans., Auto. Control. 1991. 36. (11), pp. 1241- 1253.

[8] Yoichi, H., Yasushi, T., and Yoshimasa, T.: Traction control of electric vehicle: Basic experimental results using the test EV "UOT Electric march". IEEE. Transactions on Industry Applications. Vol.34, No.5. September/October 1998. p. 1131-1138.

[9] S. Sadeghi, J. Milimonfared, M. Mirsalim, M. Jalalifar, "Dynamic Modeling and Simulation of a Switched Reluctance Motor in Electric Vehicle", in Proc,2006 ICIEA Conf.

[10] Lin, F. J., and Lee, C. C., 'Adaptive backstepping control for linear induction motor drive to track period refernces', IEE Proc. Electr. Power Appl., 2000,147, (6), pp 449-458.
[11] Yaolong, T., Chang, J., Hualin, T., 'Adaptive Backstepping Control and Friction Compensation for AC Servo with Inertia and Load Uncerainties', IEEE Trans. On Ind. Elect., Vol 50, N°5, 2003.
[12] C. E.Barbier, B. Negarede and H. L.meyer "Global Control Strategy Optimization Of An Asynchronous Drive System For An Electric Vehicle", Control Eng.Practice, vol.4.n°.8, pp.1053-1066, 1996.
[13] James Larminie, "Electric Vehicle Technology Explained", Editted by John Wiley and John Lowry, England, 2003.
[14] Benaskeur, A.R.: 'Aspects de I'application du backstepping adaptatif à la commande décentralisée des systèmes non-linéaires'. PhD thesis, Department of Electrical and Computer Engineering, Universite Laval, Quebec City, Canada, 2000.
[15] M. Krstié, I. Kanellekapolous, and P. V. Kokotovic, 'Nonlinear Design of Adaptive Controllers for Linear Systems', IEEE Trans. Automat. Contr., Vol 39, pp. 738-752, 1994.
[16] M. Ehsani, K.M. Rahman, H.A. Toliyat: Propulsion System Design of Electric and Hybrid Vehicle, IEEE Tran. On industrial Electronics, Vol. 44, No.1, February 1997.
[17] H. Huang," Electrical two speed transmission and advanced control of electric vehicles", Phd thesis, New Brunswick university, June 1998.
[18] M.Jalaliar,A.Farrokh Payam,B.Mirzaeian,and S.M.Saghaeian nezahad "Dynamic Modeling and Simulation of an Induction Motor with Adaptive Backstepping Design of an Input-Output Feedback Linearization Controller in Series Hybrid Electric Vehicle",IEEE,0-7803-9772-X-06,2002.